Supporting information

Approaching industrially relevant current densities for Hydrogen Oxidation with a bio-inspired molecular catalytic material

Jérémy Schild[†,‡], *Bertrand Reuillard*[†]*, *Adina Morozan*[†], *Pascale Chenevier*[§], *Edmond Gravel*[‡], *Eric Doris*[‡] *and Vincent Artero*[†]*

†. Univ. Grenoble Alpes, CEA, CNRS, IRIG, Laboratoire de Chimie et Biologie des Métaux, F-38000 Grenoble.

‡. Université Paris-Saclay, CEA, INRAE, Département Médicaments et Technologies pour la Santé (DMTS), SCBM, 91191 Gif-sur-Yvette, France.

§. Univ. Grenoble Alpes, CEA, CNRS, IRIG, SYMMES, F-38000 Grenoble.

*Corresponding author: vincent.artero@cea.fr ; bertrand.reuillard@cea.fr

Table of content

Experimental section

Materials and reagents

Dry (distilled) EtOH was used for the ligand synthesis. Dry solvents (MeOH, Et_2O and MeCN), for molecular synthesis, potassium phosphate salts, pyrene butyric acid ($PyCO_2H$), sulfuric acid (ACS reagent, 95-98%), dimethylformamide (DMF) were purchased from Sigma-Aldrich. The PTFE treated supporting gas diffusion layer were obtained from Sigracet (GDL 39BC). The synthesis and characterisation of the $P_2^{Cy}N_2^{Arg}$ ligand and **NiArg** was carried out as previously reported.[1]

NiArg|$PyCO_2H$|MWCNTs|GDL electrode preparation

2 mg of MWCNTs (NC700, Nanocyl) were dispersed in 40 mL of EtOH (0.05 mg mL^{-1}) for 20 minutes in an ultrasonic bath. The dispersion was then filtered directly onto a 10 cm^2 GDL disk under vacuum. This lead to the MWCNTs|GDL films with 0.2 mg cm^{-2} of MWCNTs. Without drying, the MWCNTs|GDL films were then directly soaked in DMF solutions (6 mL) containing various concentration of $PyCO_2H$ derivative (0 ; 2.5 ; 5 ; 10 ; 20 and 50 mM) for 10 min. The modified films were then soaked in 10 mL of DMF for 1 minute, in order to remove excess of unbound $PyCO_2H$ from the film. This washing step was deliberately kept short in order to minimize desorption of the adsorbed $PyCO_2H$ derivative. The film was then rinsed once more in distilled water in order to wash off DMF from the MWCNTs|GDL disk. The 10 cm^2 disk were then directly stored in milliQ water prior usage. This was important to prevent the film to dry and to become too hydrophobic to deposit the catalyst. In addition, the films were typically used within 48h in order to maximize measurements reproducibility.

Electrodes for electrochemical and electrocatalytic measurements were prepared by hole-punching a 0.125 cm^2 disk of "wet" MWCNTs|GDL. Then, after removing excess of water using paper towel, 5 µL of **NiArg** in milliQ water at various concentrations (1.25; 2.5; 5 or 10 mM) were deposited at the surface of the disk. The electrode was then let to soak for 5 min in a closed vessel to prevent drying of the deposit and thus to prevent catalyst concentration variations in the deposited volume. The disk was then rinsed in deionized water to remove loosely bound catalyst from the surface. The film could then be directly used for electrochemical measurements. For electrocatalytic HOR measurements, an additional 5 min drying step under an air extractor was applied to optimize the catalytic performances. This step was found to be crucial to obtain reproducible data and slight variations of drying time had high impact on catalytic performances (see Figure 3 and S11). This last drying step may need to be optimized according to the temperature and humidity conditions in the laboratory.

Immobilized $PyCO_2H$ quantification

Quantifications of the surface concentrations of $PyCO_2H$ onto the MWCNTs|GDL films were carried out through UV-vis measurements, using a Cary 60 UV-vis spectrometer. Absorbance spectra of diluted incubation solutions (before and after soaking the film) and the diluted rinsing solutions allowed to calculate the difference of $PyCO_2H$ in solution, before and after soaking, leading to a relatively accurate estimation of the surface bound $PyCO_2H$, for

different soaking solution concentrations. Absorbance of the peak at 314 nm was used to calculate the diluted solution concentration, using a calibration curved.

The surface concentration were estimated using directly the concentration measured by UV-vis and the following equation:

$$\Gamma_{PyCO2H} = \frac{C_i d_i V_i - (C_{pi} d_{pi} V_{pi} + C_r d_r V_r)}{\mathrm{A}}$$

With $\Gamma_{\mathrm{PyrCO2H}}$ the surface concentration of $PyCO_2H$ (mol cm^{-2}), C_i, C_{pi} and C_r the concentrations of the diluted incubation, post incubation and rinsing solutions, respectively (mol L^{-1}), d_i, d_{pi} and d_r the dilution factor of each the diluted incubation, post incubation and rinsing solutions, respectively, V_i, V_{pi} and V_r the original volumes of the incubation, post incubation and rinsing solutions, respectively and A the MWCNTs|GDL disk geometrical surface (cm^2). For the UV-vis measurements, dilution factors of 50 ; 100 , 200 ; 400 and 1000 were used for incubation and post incubation solutions at concentration of 2.5 ; 5 ; 10 ; 20 and 50 mM of $PyCO_2H$, respectively. Rinsing solutions were diluted 10 times for all concentrations of $PyCO_2H$ except at 50 mM where a 50x dilution was carried out.

Electrochemistry

Electrochemical measurements were carried out using a Biologic SP-300 potentiostat in a three-electrode configuration. An Ag/AgCl (sat. KCl, homemade) reference electrode was used in neutral pH conditions (0.2 M phosphate buffer) and an Hg/Hg_2SO_4 (0.5 M H_2SO_4, from ALS) reference electrode was used in acidic conditions (0.5 M H_2SO_4). A homemade "breathing" electrode[2] (geometrical area = 0.125 cm^2) was used as working electrode and a platinum wire as counter electrode. All experiments were carried out in electrolyte purged with argon and under a constant flow of argon or H_2 (30 mL min^{-1}) at the back of the working electrode, for electrochemical and electrocatalytic characterization, respectively. All CV experiments were carried out in triplicates. For all electrochemical measurements, iR drop compensation was applied using the iR compensation technique of EC-lab (ZIR), on a Biologic SP-300 potentiostat. The technique allows to measure R_u, the solution resistance, the latter was compensated at 85%. For all CVs, initial scanning potential was always the OCP and the scanning direction was always cathodic. Most of the scans presented showcase stabilized redox or electrocatalytic response obtained after several scans (the first scan is not shown).

Potentials for electrochemical characterization at pH 7 are given *vs.* the standard hydrogen electrode (SHE) and were calculated using the following equations:

$E_{\text{vs SHE}} = E_{\text{vs Ag/AgCl (KCl sat.)}} + 0.197\ \mathrm{V}$

Potentials for electrocatalytic testing at pH 0.3 are given *vs.* to the reversible hydrogen electrode (RHE) and were calculated using the following equations:

$E_{\text{vs RHE}} = E_{\text{vs Hg/HgSO4 (0.5M H2SO4)}} + 0.68\ \mathrm{V} + (0.059 \times \mathrm{pH})$

SEM measurements

Scanning Electron Microscopy (SEM) was performed on a Zeiss Ultra 55 microscope at an accelerating voltage of 5 kV and working distance of 5 mm.

Inductively coupled plasma atomic emission spectroscopy (ICP-AES)

Digestion of the **NiArg**|$PyCO_2H$|MWCNTs|GDL were carried out through sonication in 1 mL of 65% nitric acid for 1h and letting the resulting "dispersion" to sit overnight. The obtained solution were then sonicated for another 15 min prior to dilution of 200 µL of the digestion solution 5.8 mL of 10% nitric acid. Detection of Ni was carried out using a Shimadzu ICPE-9000 following an eight-point calibration. Each measurement was carried out in triplicate.

Calculation of ΔG_{ads} from K_{NiArg}

$$\Delta G_{ads} = -\mathrm{RT} \ln K_{NiArg}$$

Where ΔG_{ads} is the binding energy of NiArg to the modified electrode surface (kJ mol^{-1}), R the perfect gas constant (8.31 J mol^{-1} K^{-1}), T the temperature (K) and K_{NiArg} the binding constant of NiArg to the electrode surface (M^{-1})

Calculation of the electrochemically active surface area (ECSA)

The estimation of the ECSA was carried out as previously reported, by measuring the non-faradic capacitive current response of the electrode (associated with the charging of the double layer) using CVs at different scan rate.[3,4]

First, the specific capacitance (C_s, in F cm^{-2}) of a flat glassy carbon electrode (0.02 cm^2) was determined in 0.2 M potassium phosphate buffer at pH7 (Figure S11) using the equation below:

$$i_c = \nu C_S$$

Following this, the double layer capacitance (C_{DL} in F) of the $PyCO_2H$|MWCNTs|GDL films obtained at different drying time (Figure S12). The double layer charging current is the product of the scanrate and the double layer capacitance:

$$i_c = \nu C_{DL}$$

Where i_C is the capacitive current (in A), ν the scan rate (in V s^{-1}) and CDL the capacitance of the double layer (in F).

The ECSA can then be calculated by dividing the double layer capacitance of the electrode (C_{DL}) by the specific capacitance (C_S):

$$ECSA = \frac{C_{DL}}{C_S}$$

Estimation of the catalytic TOFs for HOR

The catalytic turnover frequencies were estimated assuming all the charge passed stemmed from hydrogen oxidation by the Ni catalyst at the electrode surface following electrochemical oxidation and using the following equation:

$$TOF_{NiArg} = \frac{I}{\mathrm{nF}\Gamma_{NiArg}}$$

With TOF_{NiArg}, the turnover number of NiArg for hydrogen oxidation (in s^{-1}), I the HOR current value at a given potential (A cm^{-2}), n the number of electrons involved in the transformation (2), F the Faraday constant (96485 C mol^{-1}) and Γ_{NiArg} the surface loading of NiArg (mol cm^{-2})

Activation energy

The activation energy was estimated measuring catalytic currents (obtained by CV at 0.35V vs SHE) at various temperatures and using the Arrhenius equation as follow:

$$I = \mathrm{A} - e^{\frac{-E_a}{RT}}$$

$$\ln I = \ln A - \frac{E_a}{RT}$$

With I the current density at a given potential (in A cm-2), A the pre-exponential factor, E_a is the activation energy (in J mol^{-1}), R the perfect gas constant (8.31 J mol^{-1} K^{-1}) and T the temperature (in K)

Treatment of Data

ICP-AES, CVs at pH 7 and in 0.5 M H_2SO_4 measurements (0, 5 and 8 min drying) of the NiArg|$PyCO_2H$|MWCNTs|GDL films were carried out in triplicates. Average value and standard deviation were calculated as follow:

$$x_0 = \sum_i \frac{x_i}{n} \quad \sigma = \sqrt{\sum_i \frac{(x_i - x_0)^2}{(n-1)}}$$

With n the number of experiments, x_0 the unweighted mean value and x_i the value of the a sample

Supporting table and figures

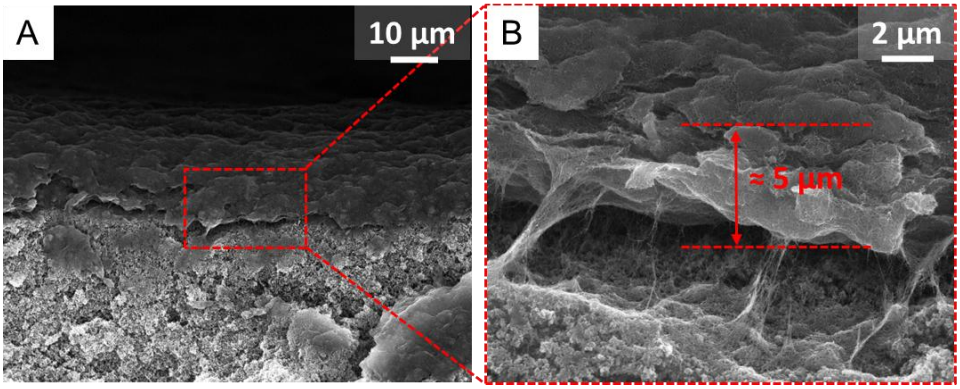

Figure S1: SEM images of the MWCNTs|GDL with A) a cross sectional view of the GDL and the MWCNTs surface and B) a zoom-in on the MWCNTs layer at the surface of the microporous layer of the GDL.

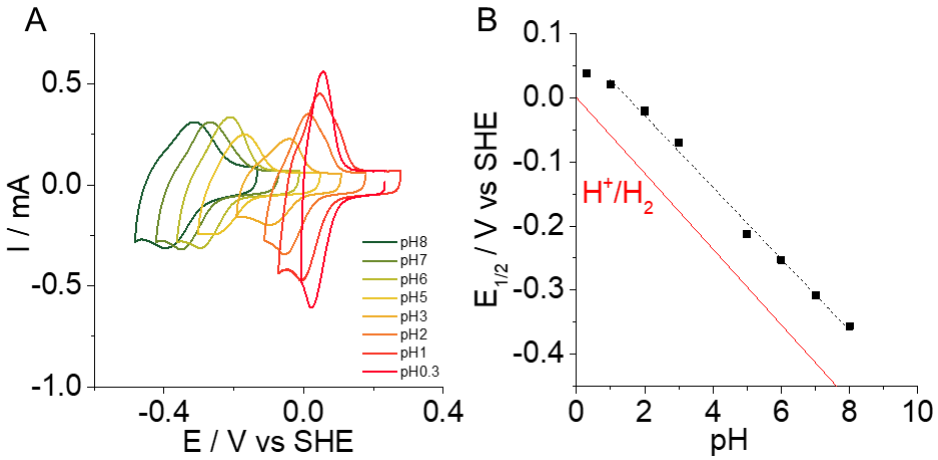

*Figure S2: A) CVs of a **NiArg**|$PyCO_2H$|MWCNTs|GDL electrodes with 10 mM $PyCO_2H$ and 10 mM **NiArg** at various pHs: potassium phosphate 0.2 M (from pH 8 to 5 included), Na_2SO_4/H_2SO_4 0.1 M (from pH 4 to 1) or 0.5 M H_2SO_4 (pH 0.3) (under Ar, 25 °C, scan rate 20 mV s^{-1}); CVs initial starting potential was the OCP and the initial scanning direction was cathodic; B) $E_{1/2}$ variations with the changes in pH obtained from CVs measurements.*

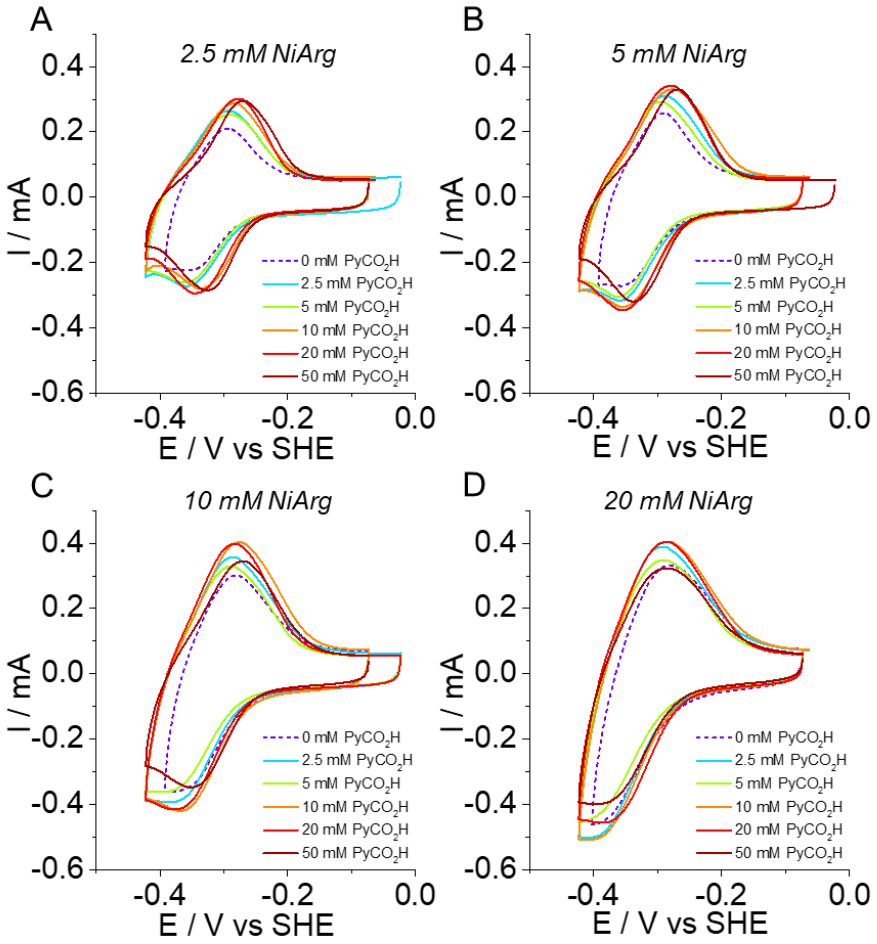

*Figure S3: CVs of **NiArg**|$PyCO_2H$|MWCNTs|GDL electrodes with different concentrations of $PyCO_2H$ (from 0 to 50 mM, from dark blue to beige curves respectively) and 5 µL **NiArg** at A) 2.5 mM B) 5mM C) 10 mM and D) 20 mM in potassium phosphate buffer 0.2 M, pH7, 25°C, under Ar, scan rate 20 mV s^{-1}; CVs initial starting potential was the OCP and the initial scanning direction was cathodic.*

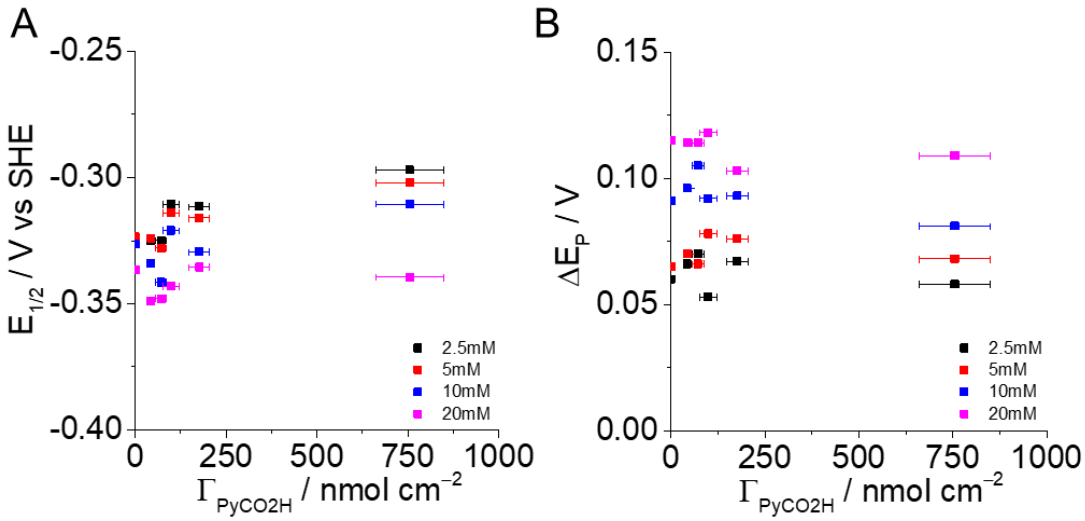

*Figure S4: Evolution of A) the $E_{1/2}$ and B) the ΔE peak of **NiArg** as function of the surface coverage in $PyCO_2H$, obtained from CV experiments at pH 7 (under Ar, 25°C).*

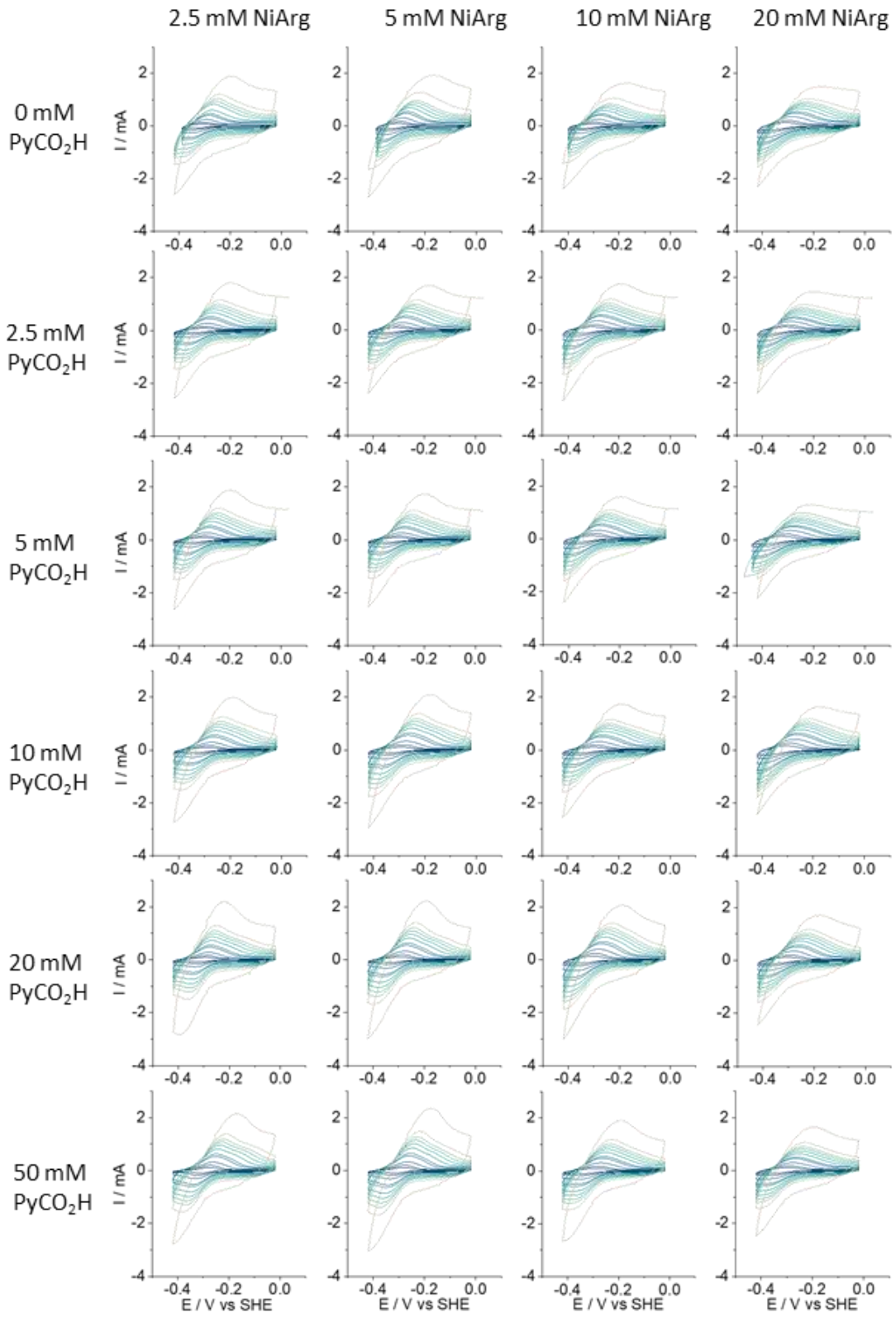

*Figure S5: CVs at various scan rate (5; 10; 20; 40; 50; 75; 100; 125; 150; 200 and 500 mV s^{-1}, traces from blue to beige) of the **NiArg**|$PyCO_2H$|MWCNTs|GDL electrodes with various concentration of $PyCO_2H$ and **NiArg** (potassium phosphate buffer 0.2 M, pH 7, under Ar, 25 °C). CVs initial starting potential was the OCP and the initial scanning direction was cathodic.*

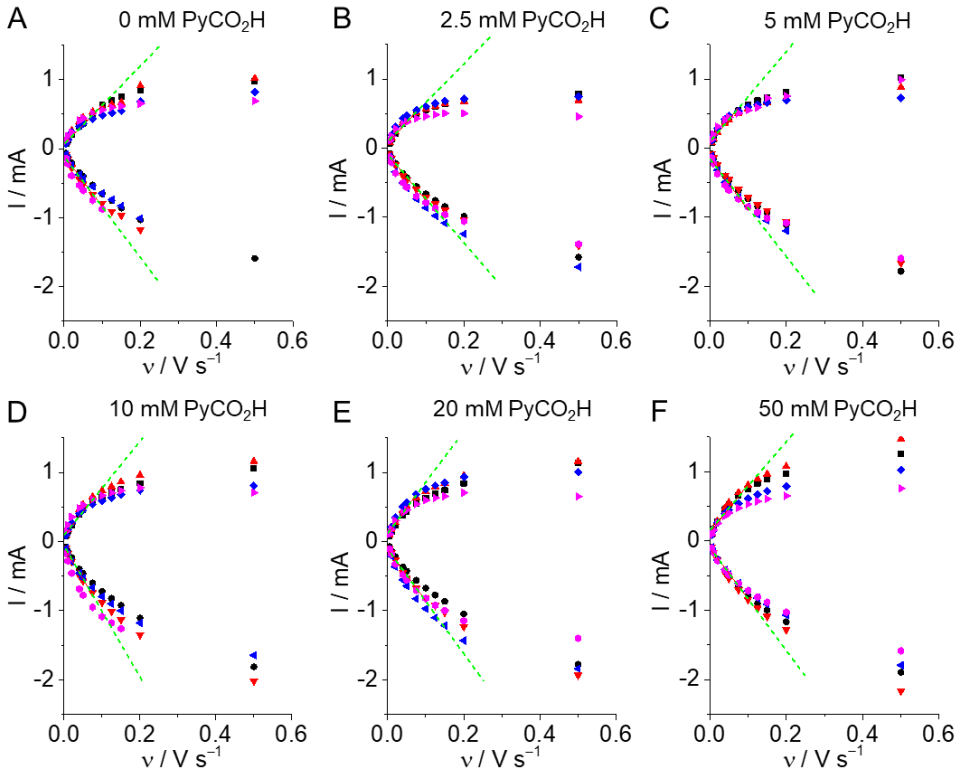

*Figure S6: Evolution of the anodic and cathodic peak currents as function of the scan rate of the electrodes with A) 0 mM B) 2.5 mM C) 5 mM D) 10 mM E) 20 mM and F) 50 mM of $PyCO_2H$ and various concentration of **NiArg**: 2.5 mM (black dots), 5 mM (red triangles), 10 mM (blue triangles) and 20 mM (purple dots) obtained from CV measurements performed at ν = 5 ; 10 ; 20 ; 40; 50; 75; 100; 125; 150; 200 and 500 mV s^{-1} (potassium phosphate 0.2 M, pH7, under Ar, at 25°C).*

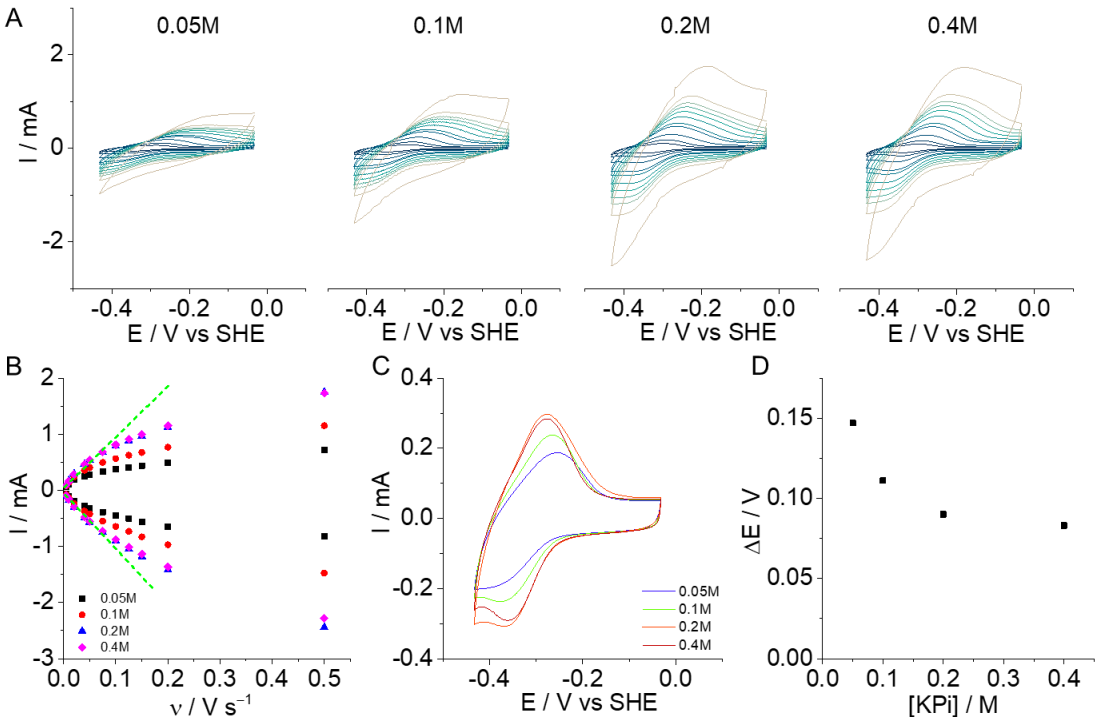

*Figure S7: A) CVs of **NiArg**|$PyCO_2H$|MWCNTs|GDL electrode (10 mM **NiArg** and 10 mM $PyCO_2H$) at various scan rate (5; 10; 20; 40; 50; 75; 100; 125; 150; 200; 500 mV s^{-1}) in potassium phosphate 0.05; 0.1; 0.2 and 0.4 M, pH7, under Ar, at 25°C; B) Evolution of the peak current with the scan rate in different potassium phosphate buffer concentration; C) CVs of the **NiArg**|$PyCO_2H$|MWCNTs|GDL electrode (10 mM **NiArg** and 10 mM $PyCO_2H$) in different potassium phosphate buffer concentrations (0.05; 0.1; 0.2 and 0.4M) under Ar, at 25°C (scan rate 20 mV s^{-1}); D) Evolution of the peak separation (ΔE) with the salinity of the buffer. CVs initial starting potential was the OCP and the initial scanning direction was cathodic.*

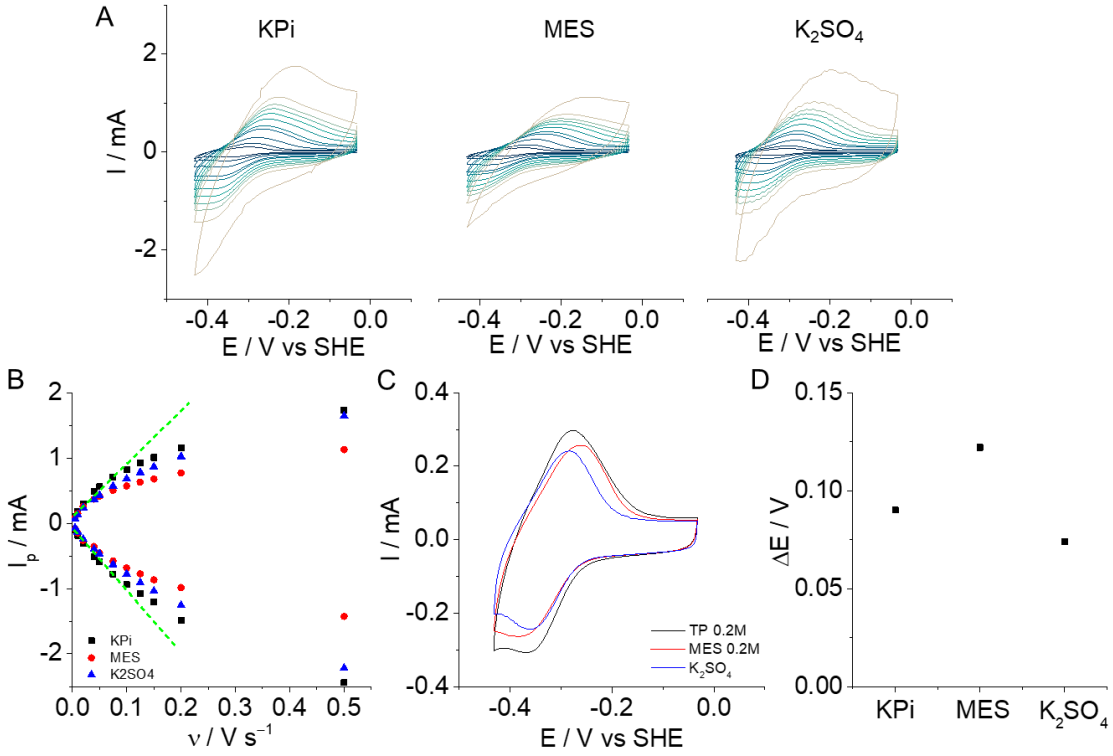

*Figure S8: A) CVs of **NiArg**|$PyCO_2H$|MWCNTs|GDL electrode (10 mM **NiArg** and 10 mM $PyCO_2H$) at various scan rate (5; 10; 20; 40; 50; 75; 100; 125; 150; 200; 500 mV s^{-1}) in various buffers (KPi, MES and K_2SO_4) 0.2 M, pH7, under Ar, at 25°C; B) Evolution of the peak current with the scan rate in different buffers; C) CVs of the **NiArg**|$PyCO_2H$|MWCNTs|GDL electrode (10 mM **NiArg** and 10 mM $PyCO_2H$) in different buffer 0.2 M, pH7, under Ar, at 25°C (scan rate 20 mV s^{-1}); D) Evolution of the peak separation (ΔE) with buffer type. CVs initial starting potential was the OCP and the initial scanning direction was cathodic.*

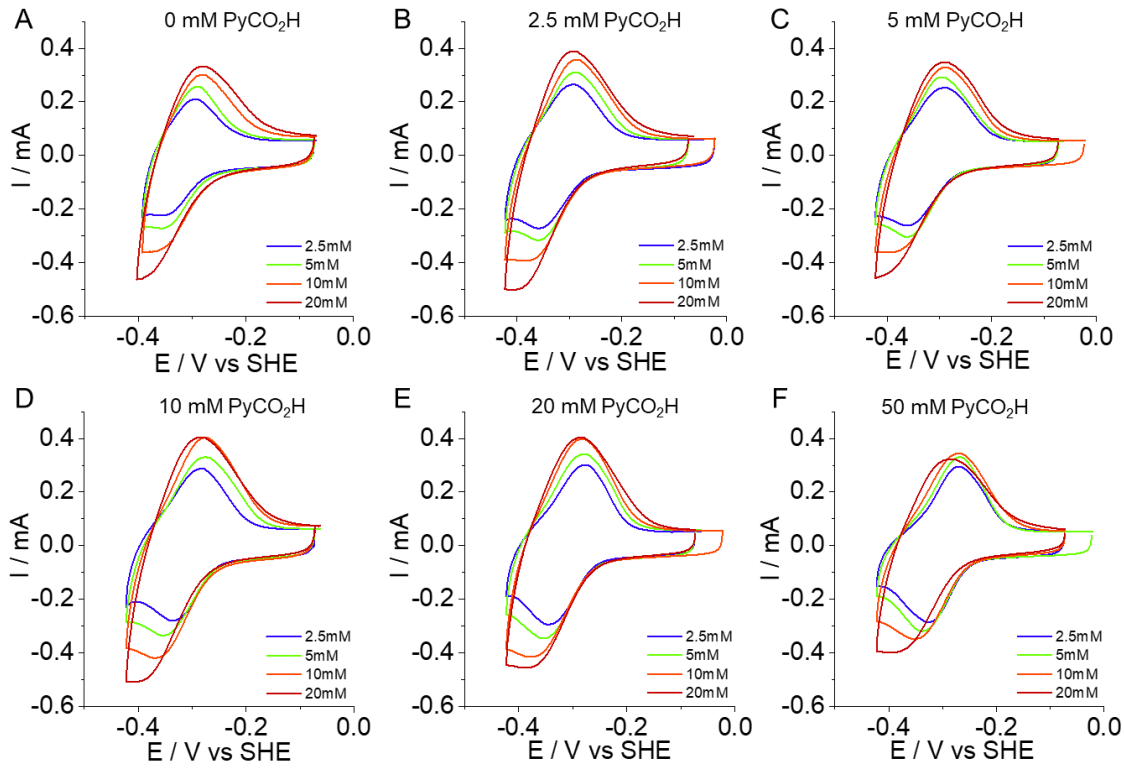

*Figure S9: CVs of the **NiArg**|$PyCO_2H$|MWCNTs|GDL electrodes with A) 0 mM B) 2.5 mM C) 5 mM D) 10 mM E) 20 mM and F) 50 mM PyCO2H and further modified with **NiArg** (2.5; 5; 10 and 20 mM) (potassium phosphate 0.2 M, pH 7, under Ar, 25°C, scan rate 20 mV s^{-1}). CVs initial starting potential was the OCP and the initial scanning direction was cathodic.*

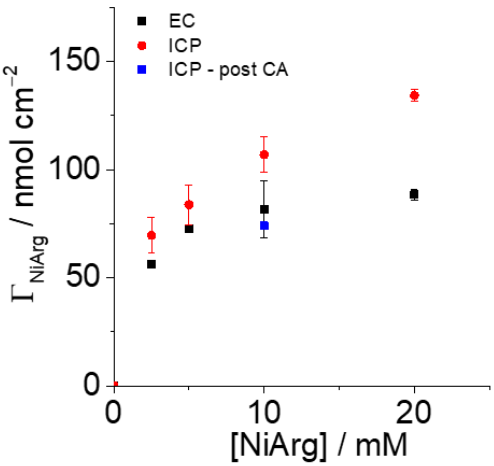

Figure S10: ***NiArg*** *surface concentrations calculated from integration of the 2-electrons oxidation wave obtained by CV measurements (black squares, phosphate buffer 0.2 M, pH 7) or from ICP-OES on acid digestion in nitric acid (65%) of the* ***NiArg****|PyCO$_2$H|MWCNTs|GDL (10 mM PyCO$_2$H, red dots) and the same* ***NiArg****|PyCO$_2$H|MWCNTs|GDL (10 mM PyCO$_2$H, dried 5 min) after 1h of CA at 0.1 V (blue square)*

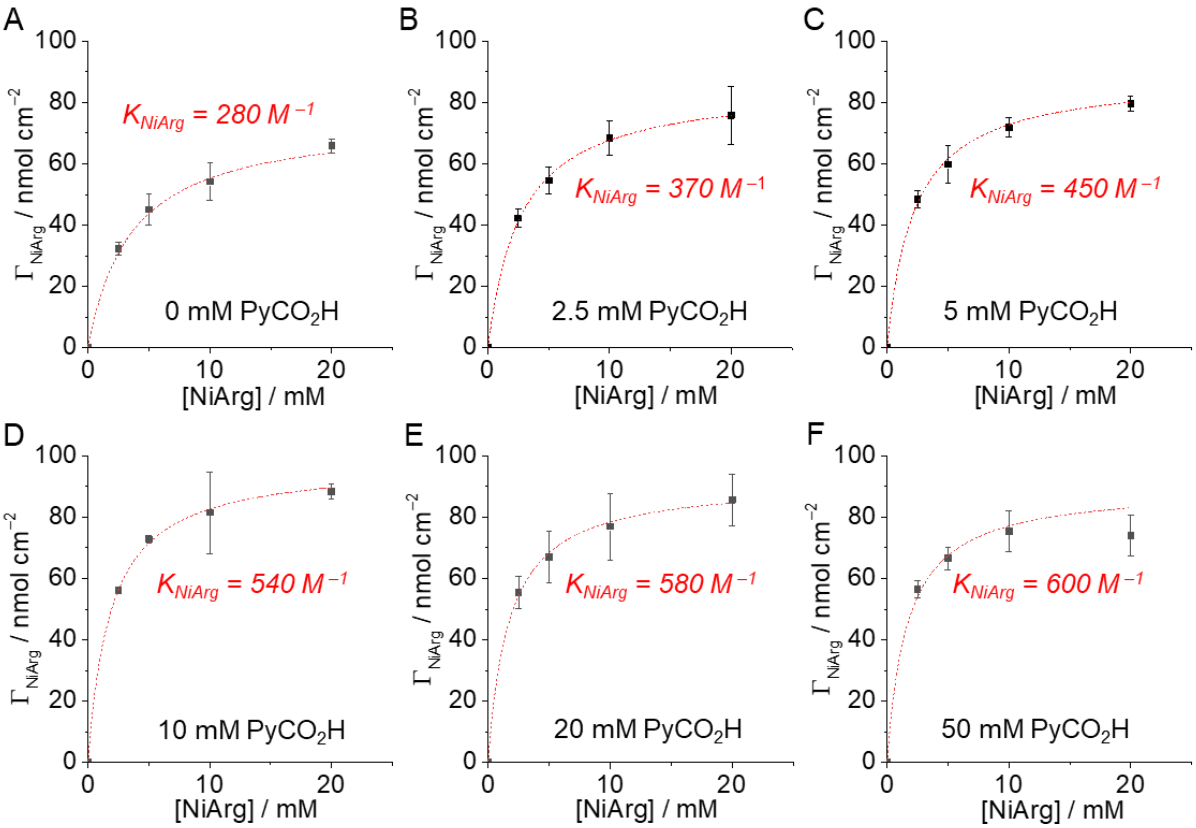

Figure S11: Evolution of Γ_{NiArg} with increasing concentration of ***NiArg*** *in the soaking solution for* ***NiArg****|PyCO$_2$H|MWCNTs|GDL electrodes with A) 0 mM B) 2.5 mM C) 5 mM D) 10 mM E) 20 mM and F) 50 mM of PyCO$_2$H. Experimental data (black squares) are fitted with a simple Langmuir binding isotherm (red dashes) allowing to access the binding constant (K_{NiArg}).*

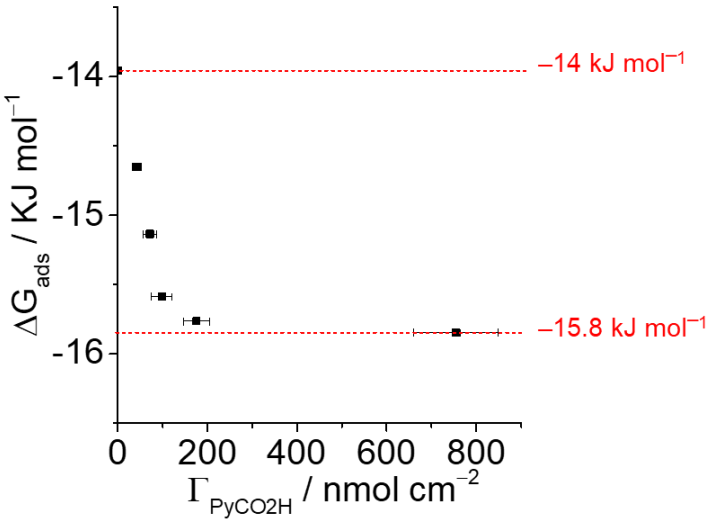

*Figure S12: Evolution of the binding energy of immobilized **NiArg** on $PyCO_2H$|MWCNTs|GDL with the surface concentration of $PyCO_2H$ anchoring sites.*

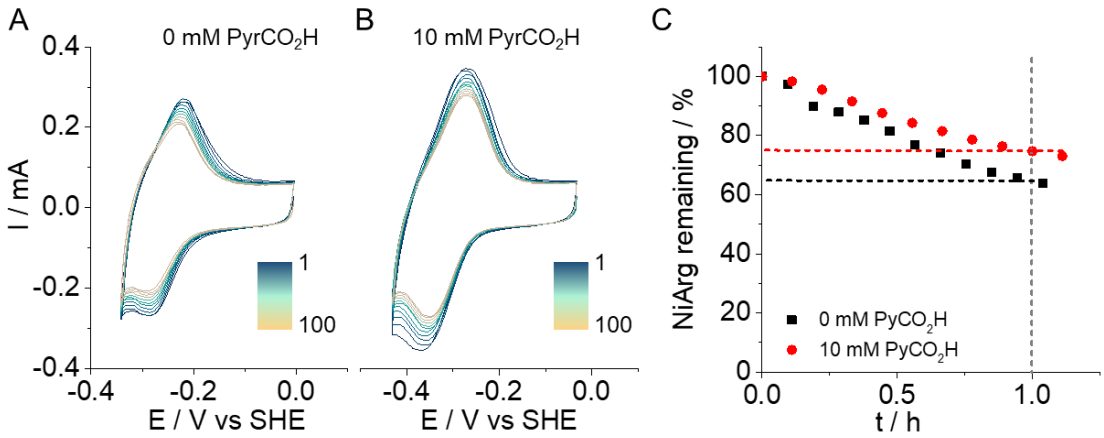

*Figure S13: CVs scans of the **NiArg**|$PyCO_2H$|MWCNTs|GDL electrodes (10 mM **NiArg**) modified with A) 0 and B) 10 mM of $PyCO_2H$ (potassium phosphate 0.2 M, pH 7, under Ar, 25°C, scan rate 20 mV s^{-1}). 100 consecutive scans were performed but the graphs only depict one out of ten cycles for clarity. C) Remaining Γ_{NiArg} overtime, from integration of the oxidation wave. CVs initial starting potential was the OCP and the initial scanning direction was cathodic.*

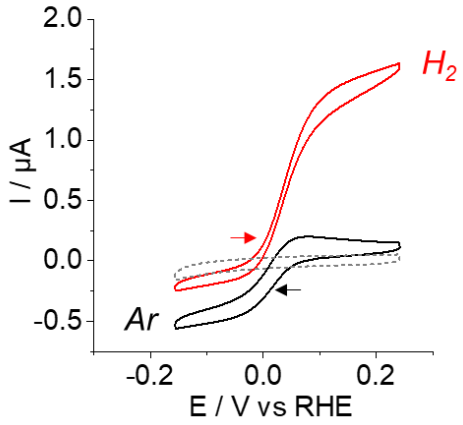

*Figure S14: CV of **NiArg** (100 µM) in 0.1 M H_2SO_4 (pH1) at 40°C under Ar or H_2 (scan rate 50 mV s^{-1}). The red and black arrows indicate the initial scanning direction*

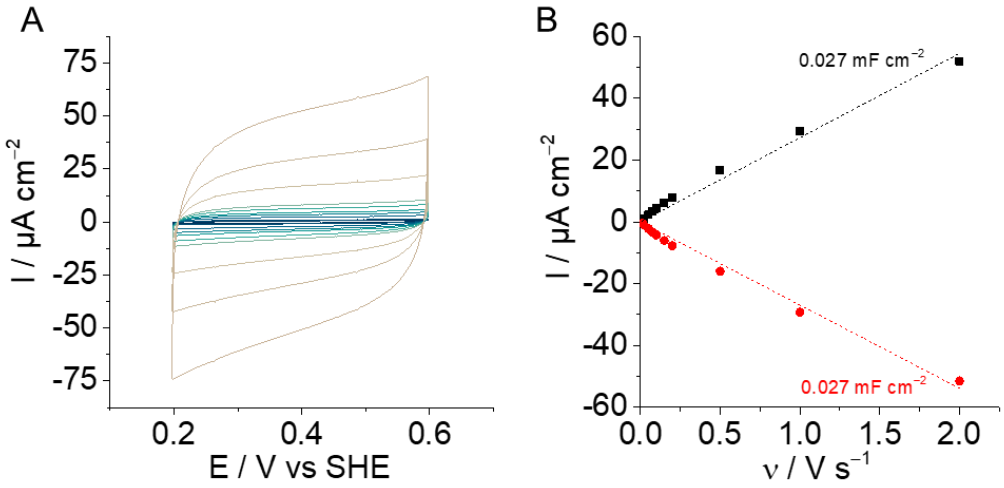

Figure S15: A) CVs at different scan rate (10; 20; 50; 75; 100; 150; 200; 500; 1000 and 2000 mV s^{-1}) in potassium phosphate buffer 0.2 M, pH 7, 25°C and B) evolution of the capacitive contribution with the scan rate of a bear and flat glassy carbon electrode (0.02 cm^2) from CVs measurements. The slope gives the specific capacitance of the flat glassy carbon electrode, Cs = 0.027 mF cm^{-2}.

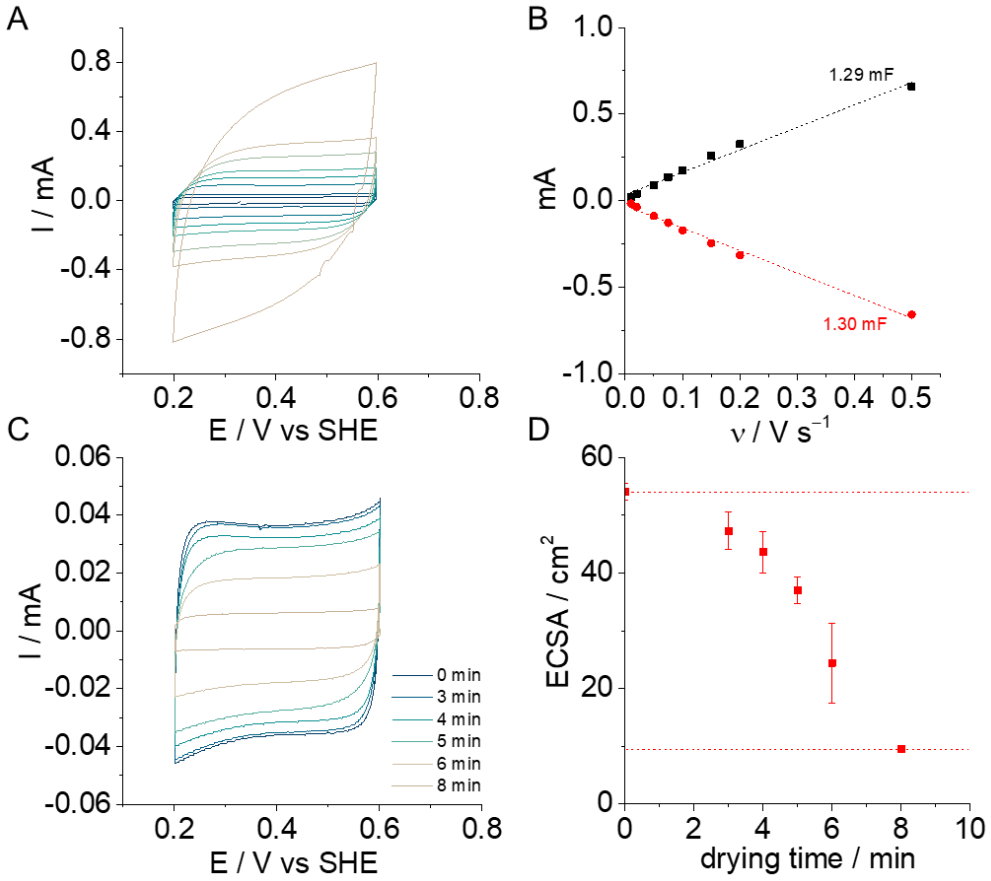

Figure S16: A) CVs at different scan rate (10; 20; 50; 75; 100; 150; 200 and 500 mV s^{-1}) in potassium phosphate buffer 0.2 M, pH7, 25°C and B) evolution of the capacitive contribution with the scan rate of $PyCO_2H$|MWCNTs|GDL electrode (0.125 cm^2 geometric) dried for 0 minutes from CVs measurements. The slope gives the double layer capacitance of the $PyCO_2H$|MWCNTs|GDL (C_{DL} = 1.29 mF); C) CVs of a $PyCO_2H$|MWCNTs|GDL electrode dried for 0; 3; 4; 5; 6 and 8 minutes in potassium phosphate buffer 0.2 M, pH 7, 25°C, scan rate 20 mV s^{-1}; D) Evolution of the calculated ECSA of the $PyCO_2H$|MWCNTs|GDL electrode with duration of the drying step.

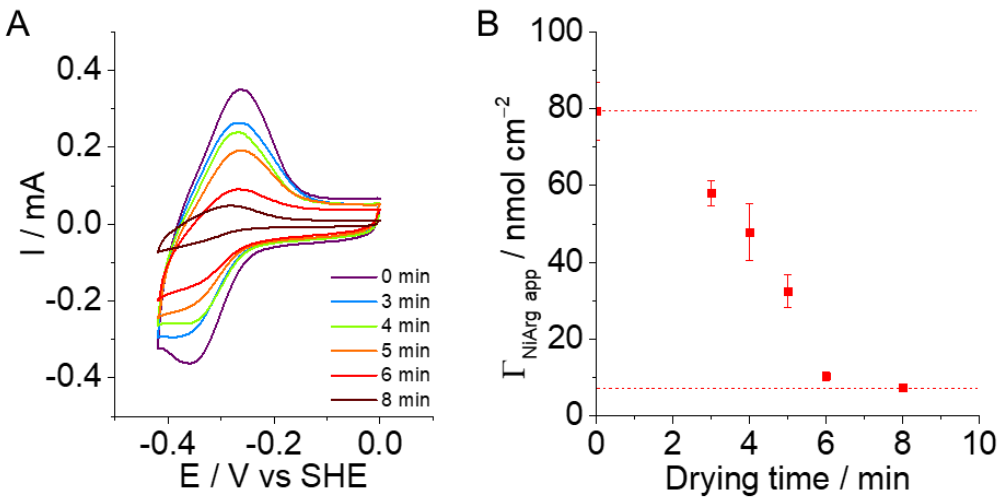

*Figure S17: A) CVs of **NiArg**|$PyCO_2H$|MWCNTs|GDL electrode with 10 mM $PyCO_2H$ and 10 mM **NiArg**, dried for 0; 3; 4; 5; 6 and 8 minutes in potassium phosphate buffer 0.2 M, pH7, 25°C (scan rate 20 mV s^{-1}). CVs initial starting potential was the OCP and the initial scanning direction was cathodic; B) Evolution of the apparent electrochemically active catalyst Γ_{NiArg} with duration of the drying step.*

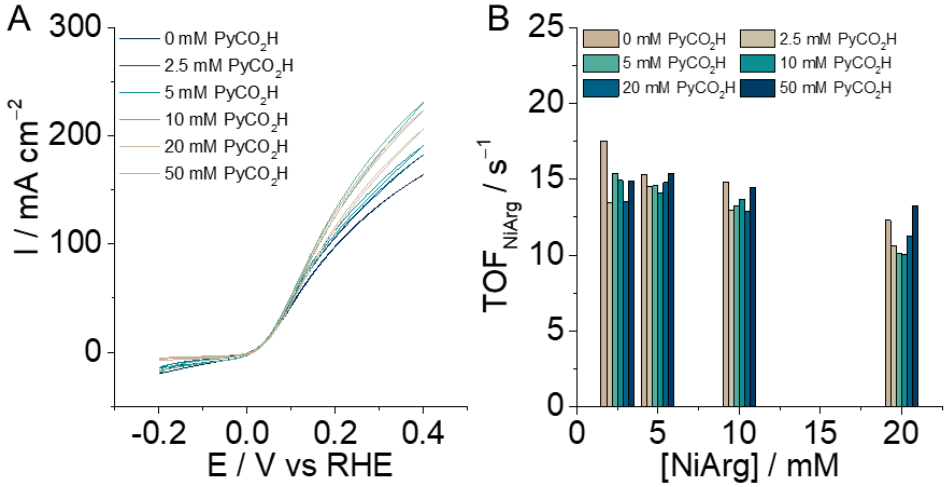

*Figure S18: A) CV of the **NiArg**|$PyCO_2H$|MWCNTs|GDL films functionalised with various concentration of $PyCO_2H$ (0; 2.5; 5; 10; 20 and 50 mM) and with 10 mM of **NiArg** after 5 min of drying time in 0.5 M H_2SO_4 degassed with argon at 25°C and with an H_2 feed at the back of the working electrode (30 mL/min) (v = 20 mV s^{-1}). CVs initial starting potential was the OCP and the initial scanning direction was cathodic; B) TOF of **NiArg** for HOR estimated from catalytic currents measured in CV, at 0.4 V overpotential*

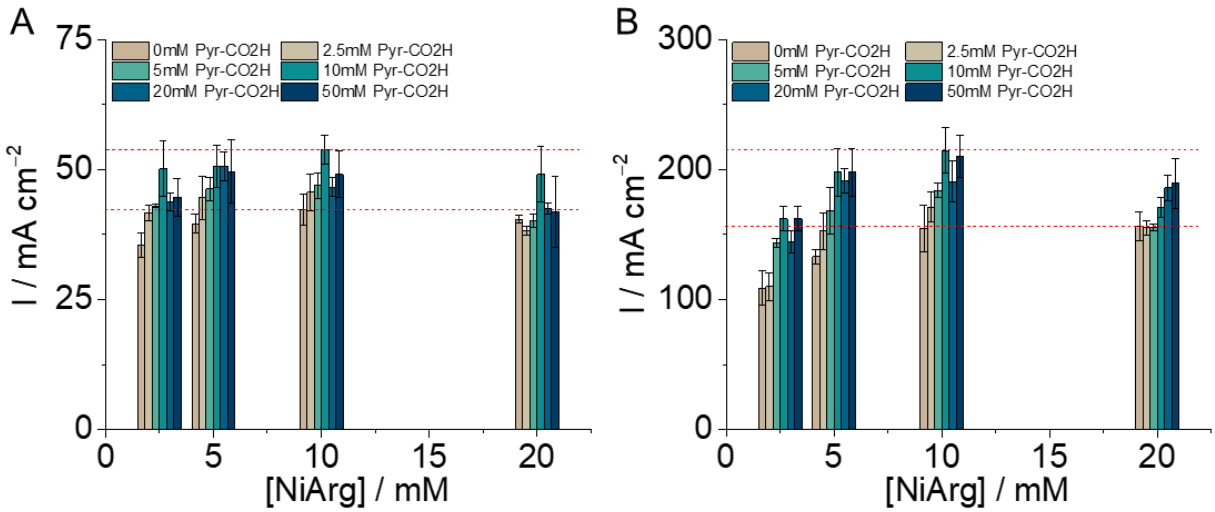

*Figure S19: Catalytic currents values for HOR at A) 0.1 V and B) 0.4 V vs RHE for all **NiArg** concentrations on $PyCO_2H$|MWCNTs|GDL obtained from CVs measurements performed in triplicates in 0.5 M H_2SO_4 (under Ar and with an H_2 feed at the back of the working electrode (30 mL/min), scan rate 20 mV s^{-1}).*

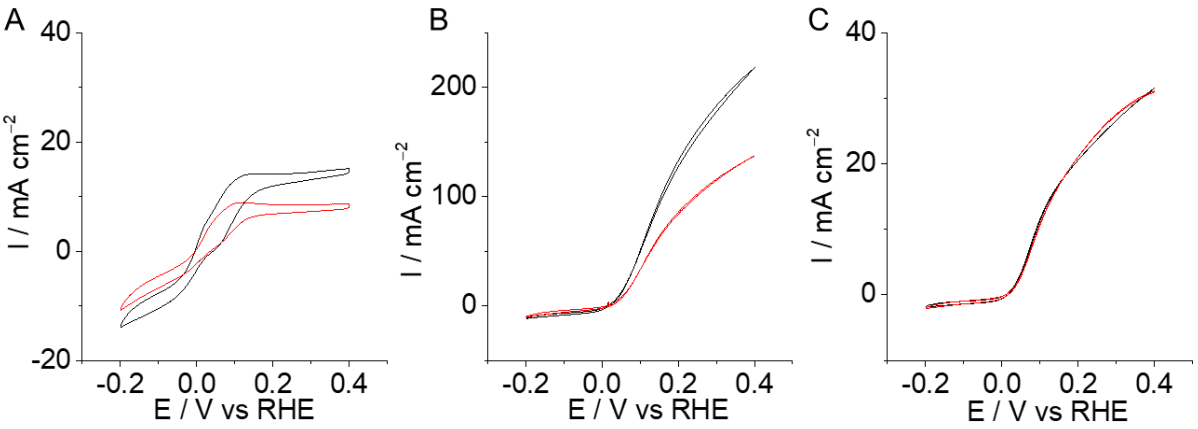

*Figure S20: CVs before (black trace) and after (red trace) chronoamperometric measurements at 0.1 V for 1 h of the **NiArg**|$PyCO_2H$|MWCNTs|GDL electrodes with 10 mM $PyCO_2H$ and 10 mM **NiArg** dried for A) 0 minutes B) 5 minutes and C) 8 minutes in 0.5 M H_2SO_4, under Ar and with an H_2 feed at the back of the working electrode (30 mL/min), at 25°C (scan rate 20 mV s^{-1}). CVs initial starting potential was the OCP and the initial scanning direction was cathodic.*

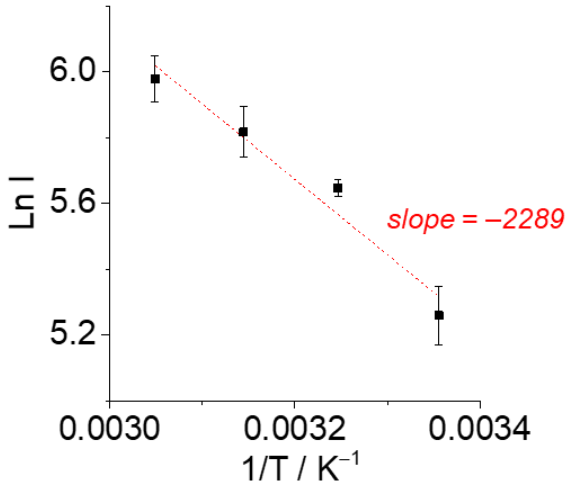

*Figure S21: Arrhenius plot of the **NiArg**|$PyCO_2H$|MWCNTs|GDL electrode with 10 mM $PyCO_2H$ and 10 mM **NiArg** taking the current densities obtained from CVs measurments in 0.5 M H_2SO_4 with H_2 feed at the back of the working electrode at 0.38 V vs SHE and at 298; 308; 318 and 328 K.*

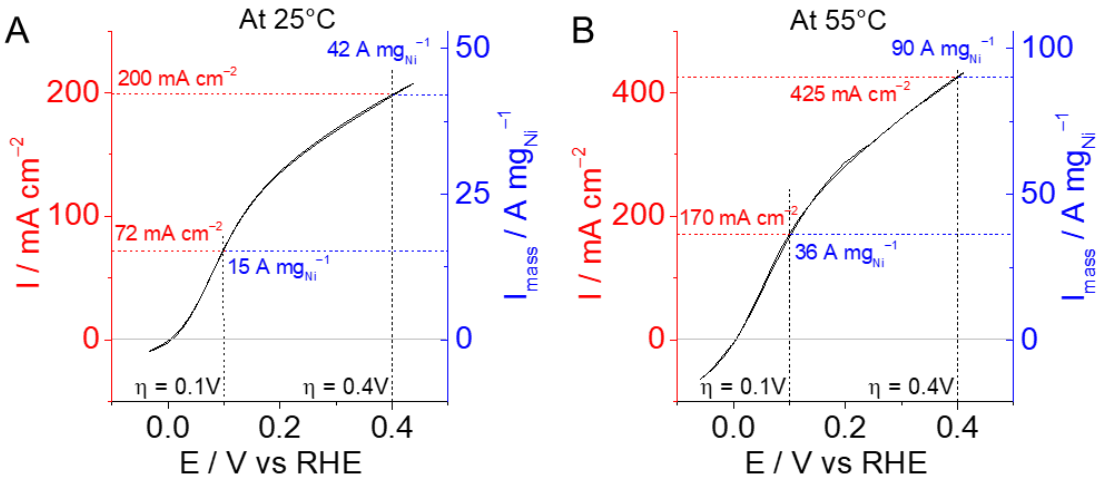

*Figure S22: CV of the **NiArg**|$PyCO_2H$|MWCNTs|GDL films functionalised with 10 mM of $PyCO_2H$ and with 10 mM of **NiArg** in 0.5 M H_2SO_4 degassed with argon at A) 25°C and B) 55°C with an H_2 feed at the back of the working electrode (30 mL/min) (v = 20 mV s^{-1})*

Supporting references

1 A. Dutta, J. A. S. Roberts and W. J. Shaw, *Angew. Chem. Int. Ed.*, 2014, **53**, 6487–6491.

2 B. Reuillard, M. Blanco, L. Calvillo, N. Coutard, A. Ghedjatti, P. Chenevier, S. Agnoli, M. Otyepka, G. Granozzi and V. Artero, *ACS Appl. Mater. Interfaces*, 2020, **12**, 5805–5811.

3 C. Wei, S. Sun, D. Mandler, X. Wang, S. Z. Qiao and Z. J. Xu, *Chem. Soc. Rev.*, 2019, **48**, 2518–2534.

4 C. C. L. McCrory, S. Jung, J. C. Peters and T. F. Jaramillo, *J. Am. Chem. Soc.*, 2013, **135**, 16977–16987.

End of Electronic Supporting Information